

# On the Backward Path Tracking Control of N-Trailer Systems

Julius Kolb, Gunter Nitzsche, Sebastian Wagner  
*Vehicle Control and Sensor Systems*  
 Fraunhofer Institute for Transportation and Infrastructure Systems IVI  
 Dresden, Germany  
 {julius.kolb, gunter.nitzsche, sebastian.wagner}@ivi.fraunhofer.de

Klaus Röbenack  
*Institute of Control Theory*  
 Technische Universität Dresden  
 Dresden, Germany  
 klaus.roebenack@tu-dresden.de

**Abstract**—This paper considers the lateral control of articulated wheeled vehicles in backward motion. The parameterized articulated vehicle is composed of a car-like truck and  $N$  passive trailers, resulting in one single steerable axle. First a nonlinear path tracking control law based on exact linearization of an offset model is reviewed and the general stability conditions of such systems are presented. Second, a stability analysis for some vehicle cases is performed, and verified in simulation. The possible application of this path tracking control law in real world articulated vehicles is discussed, and its limitations are shown.

**Index Terms**—truck-trailer, articulated vehicle, backward motion, path tracking, nonlinear control, exact linearization, stabilization

## I. INTRODUCTION

The area of autonomous driving ranges from the forward and backward motion of single vehicles to the complex maneuvering of vehicles with attached trailers. The present contribution considers the problem of the backward path tracking control of autonomous articulated vehicles. The backward motion of these systems is unstable, resulting in the commonly known *jack-knife* phenomenon, making the task of driving backwards with more than one trailer quite challenging even for experienced human drivers.

In articulated vehicles, often single-axle mobile robots are considered as the tractor vehicles [1]. Whereas to represent real world vehicles with Ackermann steering geometry, modeling is done through car-like tractors. The class of robots studied in this contribution are truck-trailer mobile robots, composed of a car-like robot and a number  $N$  of passive, i.e., non-steered, trailers. Their physical interconnection can be on-axle or off-axle w.r.t. the preceding vehicles' rear axle, defining the hitch point position. A common practice [2] is to distinguish vehicles between General N-Trailer (GNT), Standard N-Trailer (SNT) and non-Standard N-Trailer (nSNT), see Table I for the classification and Fig. 2 for a graphical example.

TABLE I  
ARTICULATED VEHICLE CLASSIFICATION

Type	Hitch point location
General N-Trailer (GNT)	on- and off-axle
Standard N-Trailer (SNT)	on-axle
non-Standard N-Trailer (nSNT)	off-axle

The reverse motion of articulated vehicles is widely studied in literature [1], [3]–[5]. In [3], the SNT System is proven to be flat considering a special linearizing output. A comparison study between nonlinear and model-free control is done in [6] and shows promising results for avoiding difficult kinetic modeling with its problematic parameter deviations. A qualitative overview of different control approaches is shown in [7].

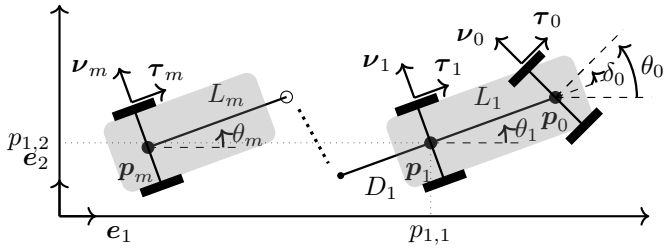
This work extends [8], and therefore continues the review of the control laws discussed in [9]–[12]. In the first approach, the nSNT vehicle was considered and transformed via a virtual vehicle into a SNT vehicle in order to apply exact input-state linearization on that virtual vehicle, obtaining the control law. In the cited articles, a solution for the path tracking problem for some types of tractor-trailer vehicles was found. However, clear limitations of these methods appear when considering widely used real commercial road vehicles, like semi-trailers and road-trains.

## II. KINEMATIC VEHICLE MODEL

This section presents the models of a generalized articulated vehicle used. In order to get an insight into the control problem in real commercial truck trailer systems, these models are fully parameterized to resemble the different structure types found in real vehicles. The studied vehicle is composed of a car-like tractor and  $N$  passive trailers, i.e., their wheels are non-steerable. Since the movements cover low speed maneuvers on flat surfaces, a kinematic model is sufficient for the study.

Regarding the generality of the model depicted in Fig. 1, parameter  $D$  changes the hitch point position of the next trailer with respect to the previous one, in order to represent the different types of real vehicles, including semi-trailers and road-trains. Fig. 2 shows the convention used for the values of  $D$ . For on-axle configurations,  $D$  is set to zero. There are two off-axle cases, with negative offset  $D < 0$ , if the hitch point is in front of the axle, and positive offset  $D > 0$ , if behind. As will be shown in Section III, the hitch point position with respect to the axle center is crucial for the considered control problem.

Two vehicle models are described: the fixed-frame model, which describes the vehicle movement on a plane and is employed in the simulation, and the offset model, used in the control algorithm.


 Fig. 1. General  $N$ -Trailer-System with car-like tractor.

### A. Fixed frame model

The derivation of kinematic vehicle models is vastly described in literature, e.g. [10]. In this contribution, a compact vector notation [1] is used for the models. The vehicle model of a General  $N$ -Trailer-System with a car-like tractor in a fixed Cartesian reference system is shown in Fig. 1. Since the number of trailers is  $N$ , the total number of bodies is  $m = N + 1$ . The front axle of the car-like tractor is steered and indexed by 0.

The position of the axle centers on the plane are  $p_0 \dots p_m$ , with the components  $(p_{i,1}, p_{i,2})$ , and the orientation of the axles is described by  $\theta_0 \dots \theta_m$ .  $L_1$  is the wheelbase,  $L_2 \dots L_m$  is the distance from the hitch point to the wheel axle of the trailers. The parameter  $D$  was previously defined and has to be specified for  $D_1 \dots D_{m-1}$ .

By introducing the tangential vector  $\tau_i = \cos \theta_i e_1 + \sin \theta_i e_2$  and the normal vector  $\nu_i = -\sin \theta_i e_1 + \cos \theta_i e_2$ , and after short calculations, the kinematic model equations follow as

$$\dot{p}_{1,1} = v_1 \cos \theta_1 \quad (1)$$

$$\dot{p}_{1,2} = v_1 \sin \theta_1 \quad (2)$$

$$\omega_1 = (v_1/L_1) \tan \delta_0 \quad (3)$$

$$\omega_i = (1/L_1) [v_1 \langle \tau_1, \nu_i \rangle - \sum_{j=2}^{i-1} (L_j + D_j) \omega_j \langle \nu_j, \nu_i \rangle - D_1 \omega_1 \langle \nu_1, \nu_i \rangle], \quad i = 2, \dots, m, \quad (4)$$

with the translational velocity  $v_i = \dot{p}_i = v_i \tau_i$  and the rotational velocity  $\dot{\theta}_i = \omega_i$ . Notice the scalar product notation  $\langle \cdot, \cdot \rangle$  used. Let us define here the system state as  $\mathbf{x} = (p_{1,1}, p_{1,2}, \omega_1, \dots, \omega_m)^T$ .

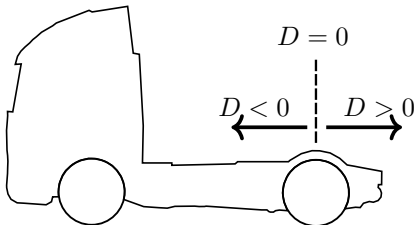


Fig. 2. Convention for hitch point position.

The relation between two consecutive body axle center positions follows from geometric constraints and is

$$p_i = p_{i+1} + L_{i+1} \tau_{i+1} + D_i \tau_i. \quad (5)$$

Finally, the relative orientation of two consecutive bodies to one another is described by  $\phi_i = \theta_i - \theta_{i+1}$  for  $i = 1, \dots, m-1$ .

Taking the time derivative of (5), the velocity propagation between two consecutive vehicle bodies can be obtained and written in matrix notation as

$$\begin{pmatrix} v_{i+1} \\ \omega_{i+1} \end{pmatrix} = \underbrace{\begin{pmatrix} \cos \phi_i & D_i \sin \phi_i \\ \frac{1}{L_{i+1}} \sin \phi_i & -\frac{D_i}{L_{i+1}} \cos \phi_i \end{pmatrix}}_{{}^{i+1}M_i \in \mathbb{R}^{2 \times 2}} \begin{pmatrix} v_i \\ \omega_i \end{pmatrix}. \quad (6)$$

This represents the front-to-back propagation. For the inverse relation,  $D_i \neq 0$  is needed in order to prevent a singular matrix, obtaining

$$\begin{pmatrix} v_i \\ \omega_i \end{pmatrix} = \underbrace{\begin{pmatrix} \cos \phi_i & L_{i+1} \sin \phi_i \\ \frac{1}{D_i} \sin \phi_i & -\frac{L_{i+1}}{D_i} \cos \phi_i \end{pmatrix}}_{{}^iM_{i+1}} \begin{pmatrix} v_{i+1} \\ \omega_{i+1} \end{pmatrix}. \quad (7)$$

The back-to-front velocity propagation for cases where at least one  $D = 0$  is treated in different ways, e.g. [1], [13].

### B. Offset model

For the path-tracking task, it is customary to describe the movement with respect to the path, since it simplifies the control problem. Modeling of path-dependent relations is described e.g. in [1], [10], [14], [15].

In order to develop the offset relations, we introduce the equivalent virtual steering axles and their angles in the hitch points that describe the current body movement in Fig. 3. Note that from (3) and with the virtual steering axles, the relation

$$\dot{\theta}_i = \frac{v_i}{L_i} \tan \delta_{i-1} \quad (8)$$

follows for each body.

For the backward path tracking, it is convenient to take axle  $p_m$  of the last trailer as the reference point of the vehicle. Fig. 4 shows the last trailer with the relations to the

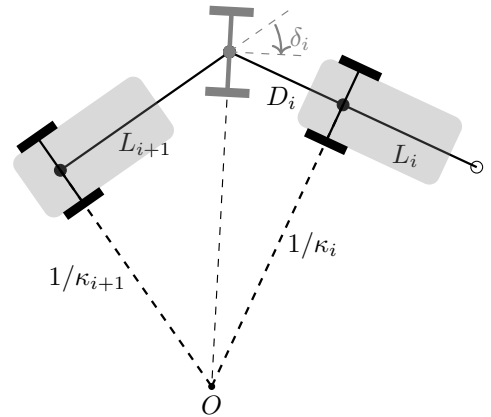


Fig. 3. Definition virtual steering axle and angle in grey.

path. Newly introduced symbols are the curvilinear distance  $s$  along the path, the curvature  $\kappa$  of the path as well as the instantaneous center  $O(s_d)$  of the resulting desired circle. Subscript  $d$  denotes the desired values. Therefore, the desired path point is  $\mathbf{p}_d = \mathbf{p}_p(s_d)$ .

The offset parameters are the off-track-distance  $d_{os}$  and the orientation errors  $\theta_{os}$  and  $\phi_{os,i}$ ,

$$d_{os} = (p_{m,1} - p_{d,1}) \sin \theta_d + (p_{m,2} - p_{d,2}) \cos \theta_d \quad (9)$$

$$\theta_{os} = \theta_m + \pi - \theta_d \quad (10)$$

$$\phi_{os,i} = \phi_i - \phi_d, \quad i = 1, \dots, m-1. \quad (11)$$

Since  $\mathbf{p}_m$  lies on the axis described by  $\nu_d$ , one gets the relation  $\langle \mathbf{p}_m - \mathbf{p}_d, \tau_d \rangle = 0$ , from which we can obtain the relative velocity with respect to the desired path point,

$$\dot{s}_d = -\frac{v_m \cos \theta_{os}}{1 - d_{os} \kappa_{d,m}}. \quad (12)$$

The off-track distance dynamics is obtained by taking the derivative of  $d_{os}^2 = \|\mathbf{p}_m - \mathbf{p}_d\|_2^2 = \langle \mathbf{p}_m - \mathbf{p}_d, \mathbf{p}_m - \mathbf{p}_d \rangle$ . Finally, the time-dependent offset differential equations follow as

$$\dot{d}_{os} = -v_m \sin \theta_{os} \quad (13)$$

$$\dot{\theta}_{os} = \dot{\theta}_m - \dot{\theta}_d = \dot{\theta}_m - \frac{d\theta_d}{ds_d} \dot{s}_d = \omega_m + \kappa_{d,m} \dot{s}_d \quad (14)$$

$$\dot{\phi}_{os,i} = \dot{\phi}_i - \dot{\phi}_{d,i} \approx \dot{\phi}_i = \dot{\theta}_i - \dot{\theta}_{i+1} = \omega_i - \omega_{i+1}. \quad (15)$$

Note the approximation done in Eq. (15). It follows from the assumption that feasible paths are built from path segments with constant curvature and only small changes in curvature are allowed in the transients, i.e.,  $\dot{\phi}_{d,i} \approx 0$ .

In order to avoid singularities, it is a common practice to express the motion equations as time-independent, i.e., depending on a path variable  $s$ . Expressing derivatives in that path variable can be easily performed by the chain rule.

For the present case, the following time-independent model equations are obtained, and derivation can be followed from

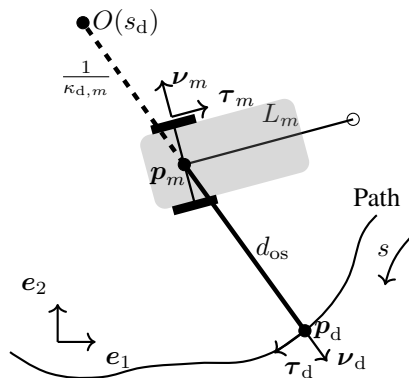


Fig. 4. Offset relations backward motion of last trailer w.r.t. path.

upper equations and [10], [15],

$$d'_{os} = (1 - d_{os} \kappa_{d,m}) \tan \theta_{os} \quad (16)$$

$$\theta'_{os} = -\frac{1 - d_{os} \kappa_{d,m}}{L_m \cos \theta_{os}} \tan \delta_{m-1} + \kappa_{d,m} \quad (17)$$

$$\phi'_{os,i} = -\frac{1 - d_{os} \kappa_{d,m}}{v_m \cos \theta_{os}} \frac{v_{i+1}}{D_i L_{i+1}} [L_{i+1} \sin \phi_i - (D_i + L_{i+1} \cos \phi_i) \tan \delta_i], \quad i = 1, \dots, m-1. \quad (18)$$

The singularities constrain the vehicle dimensions,  $L_i \neq 0$  and  $D_i \neq 0$ , as well as the orientation error

$$\cos \theta_{os} \neq 0 \Rightarrow \theta_{os} \notin \left\{ \frac{\pi}{2} + k\pi, k \in \mathbb{Z} \right\}. \quad (19)$$

### III. CONTROL PROBLEM

Since path tracking, in which the lateral deviation of the vehicle with respect to the desired path is controlled, is considered here, longitudinal errors are not analyzed.

The remaining control variable is the steering angle  $\delta_0$  of the car-like tractor vehicle. The velocity is set to a value of  $v_1 < 0$  for backward movement. Since the virtual steering angles can be propagated through the vehicle structure with (7), one can set as a fictive system input the tangent of the virtual steering angle of the last trailer,  $u_{os} = \tan \delta_{m-1}$ . Introducing the state  $\mathbf{x}_{os} = (x_{os,1}, \dots, x_{os,n})^T = (d_{os}, \theta_{os}, \phi_{os,1}, \dots, \phi_{os,m-1})^T$  of dimension  $n = m + 1$  leads to the following nonlinear offset system,

$$\mathbf{x}'_{os} = \mathbf{f}(\mathbf{x}_{os}) + \mathbf{g}(\mathbf{x}_{os}) u_{os} \quad (20)$$

$$y_{os} = h(\mathbf{x}_{os}), \quad (21)$$

with

$$\mathbf{f}(\mathbf{x}_{os}) = \begin{pmatrix} (1 - x_{os,1} \kappa_{d,m}) \tan x_{os,2} \\ \kappa_{d,m} \\ x'_{os,3}(\mathbf{x}_{os}) \\ \vdots \\ x'_{os,n-1}(\mathbf{x}_{os}) \\ -\frac{1 - x_{os,1} \kappa_{d,m}}{D_{m-1} \cos x_{os,2}} \sin(x_{os,n} + \phi_{d,m-1}) \end{pmatrix}, \quad (22)$$

$$\mathbf{g}(\mathbf{x}_{os}) = \begin{pmatrix} 0 \\ -\frac{1 - x_{os,1} \kappa_{d,m}}{L_m \cos x_{os,2}} \\ 0 \\ \vdots \\ 0 \\ \frac{1 - x_{os,1} \kappa_{d,m}}{D_{m-1} L_m \cos x_{os,2}} [D_{m-1} \cdots \\ \cdots + L_m \cos(x_{os,n} + \phi_{d,m-1})] \end{pmatrix} \quad (23)$$

and  $h(\mathbf{x}_{os}) = x_{os,1}$ , i.e., the output of the system is set to the off-track distance  $y_{os} = x_{os,1} = d_{os}$ . The symbols  $\mathbf{f}, \mathbf{g} : \mathcal{M} \rightarrow \mathbb{R}^n$  represent vector fields and  $h : \mathcal{M} \rightarrow \mathbb{R}$  is a scalar field, with the open subset  $\mathcal{M} \subseteq \mathbb{R}^n$ .

For this system, a stable backward path tracking controller is designed by applying the exact linearization technique. Therefore, the task can be expressed as  $\lim_{t \rightarrow \infty} \mathbf{x}_{os}(t) = \mathbf{0}$ .

An equilibrium of the system is, for instance, a movement on a circle, following  $\mathbf{x}_{os} = \mathbf{0}$ . Geometrically, regarding Fig. 3, one obtains the following relations for that steady state regime:

$$\frac{1}{\kappa_i} = \frac{1}{\kappa_{i+1}} \cos \phi_i + L_{i+1} \sin \phi_i \quad (24)$$

and

$$\omega_{i+1} = \omega_i \Rightarrow v_{i+1} \kappa_{d,i+1} = v_i \kappa_{d,i}. \quad (25)$$

From the system equations for the steady state movement

$$\mathbf{0} = \mathbf{f}(\mathbf{0}) + \mathbf{g}(\mathbf{0})u_{os}, \quad (26)$$

the relation for the input in that state is

$$u_{os} = \tan \delta_{m-1} = \kappa_{d,m} L_m, \quad (27)$$

and the relation for the relative angles follows as

$$0 = L_{i+1} \sin \phi_i - (D_i + L_{i+1} \cos \phi_i) \tan \delta_i. \quad (28)$$

For the exact linearization, one needs to obtain a well-defined relative degree, [16]–[18]. The relative degree is the smallest derivative order of the output that depends explicitly on the input.

A compact form of representation involves Lie derivatives. Basic definitions are the Lie derivative of a scalar field  $h$  along a vector field  $\mathbf{f}$

$$\mathcal{L}_{\mathbf{f}} h(\mathbf{x}) = dh(\mathbf{x})\mathbf{f}(\mathbf{x}) = \langle dh, \mathbf{f} \rangle(\mathbf{x}) = \sum_{i=1}^n \frac{\partial h}{\partial x_i} \mathbf{f}_i(\mathbf{x}), \quad (29)$$

obtaining again a scalar field. From the differentiation  $dh(\mathbf{x})$  a gradient results

$$dh(\mathbf{x}) = \frac{\partial h}{\partial \mathbf{x}}(\mathbf{x}) := \left( \frac{\partial h}{\partial x_1}(\mathbf{x}), \dots, \frac{\partial h}{\partial x_n}(\mathbf{x}) \right). \quad (30)$$

Computing multiple Lie derivatives along the same vector field  $\mathbf{f}$  yields to the recursion

$$\mathcal{L}_{\mathbf{f}}^k h(\mathbf{x}) = \frac{\partial \mathcal{L}_{\mathbf{f}}^{k-1} h(\mathbf{x})}{\partial \mathbf{x}} \mathbf{f}(\mathbf{x}) \quad \text{with} \quad \mathcal{L}_{\mathbf{f}}^0 h(\mathbf{x}) = h(\mathbf{x}). \quad (31)$$

For a further vector field  $\mathbf{g}$ , mixed Lie derivatives are obtained

$$\mathcal{L}_{\mathbf{g}} \mathcal{L}_{\mathbf{f}} h(\mathbf{x}) = \frac{\partial \mathcal{L}_{\mathbf{f}} h(\mathbf{x})}{\partial \mathbf{x}} \mathbf{g}(\mathbf{x}). \quad (32)$$

For complicated systems, these Lie derivatives can be computed with high efficiency by algorithmic differentiation [19].

Taking the path parameter derivative of the output yields

$$\begin{aligned} y'_{os} &= \mathcal{L}_{\mathbf{f}} h(\mathbf{x}_{os}) + \mathcal{L}_{\mathbf{g}} h(\mathbf{x}_{os})u_{os} \\ &= d'_{os} = (1 - x_{os,1} \kappa_{d,m}) \tan x_{os,2} \end{aligned} \quad (33)$$

and since the output does not appear in the equation, another derivative is needed,

$$\begin{aligned} y''_{os} &= \mathcal{L}_{\mathbf{f}}^2 h(\mathbf{x}_{os}) + \mathcal{L}_{\mathbf{g}} \mathcal{L}_{\mathbf{f}} h(\mathbf{x}_{os})u_{os} \\ &= (1 - x_{os,1} \kappa_{d,m}) \kappa_{d,m} - \frac{(1 - x_{os,1} \kappa_{d,m})^2}{L_m \cos^3 x_{os,2}} u_{os}. \end{aligned} \quad (34)$$

The system has a well-defined relative degree of  $r = 2$  for  $L_m \neq 0$ ,  $x_{os,1} \neq 1/\kappa_{d,m}$  and  $x_{os,2} \notin \{\frac{\pi}{2} + k\pi, k \in \mathbb{Z}\}$ . For practical applications, to avoid collisions with obstacles, the off-track distance of the axle center of the last trailer should be small enough and the orientation error should be  $x_{os,2} \ll \frac{\pi}{2}$ .

By defining a new input  $v$

$$y''_{os} = \mathcal{L}_{\mathbf{f}}^2 h(\mathbf{x}_{os}) + \mathcal{L}_{\mathbf{g}} \mathcal{L}_{\mathbf{f}} h(\mathbf{x}_{os})u_{os} =: v, \quad (35)$$

the linearizing feedback results as

$$u_{os} = \frac{1}{\mathcal{L}_{\mathbf{g}} \mathcal{L}_{\mathbf{f}} h(\mathbf{x}_{os})} (v - \mathcal{L}_{\mathbf{f}}^2 h(\mathbf{x}_{os})). \quad (36)$$

Since the system has a relative degree  $r < n$ , the system is input-output linearizable. Internal dynamics exist and they will determine the stability of the overall system [20].

In order to further analyze the system, one option is to compute the Byrnes-Isidori Normal Form as described in [16] or by the direct method proposed in [18]. This would split the system in two parts: The first subsystem is linearizable by feedback and the second system represents the internal dynamics, not directly dependent of the input.

Having this structure allows finally to analyze the internal dynamics. Since this process involves many computations, an alternative approach based on the original system (20) can be followed [17]. Taking the linearizing feedback (36) and choosing  $v$  as

$$v = - \sum_{k=0}^{r-1} a_k \mathcal{L}_{\mathbf{f}}^k h(\mathbf{x}) \quad (37)$$

and placing  $r$  zeros  $s_1, \dots, s_r$  on the open left half plane in

$$\prod_{i=1}^r (s - s_i) \stackrel{!}{=} s^r + a_{r-1} s^{r-1} + \dots + a_1 s + a_0, \quad (38)$$

we obtain the coefficients  $a_k$  using Vieta's formulas and  $r = 2$ :

$$a_0 = s_1 s_2 \quad (39)$$

$$a_1 = -(s_1 + s_2). \quad (40)$$

Finally, a stabilizing feedback results

$$\begin{aligned} u_{os} &= \frac{-1}{\mathcal{L}_{\mathbf{g}} \mathcal{L}_{\mathbf{f}} h(\mathbf{x}_{os})} [a_0 h(\mathbf{x}_{os}) + a_1 \mathcal{L}_{\mathbf{f}} h(\mathbf{x}_{os}) + \mathcal{L}_{\mathbf{f}}^2 h(\mathbf{x}_{os})] \\ &= \frac{L_m \cos^3 x_{os,2}}{(1 - x_{os,1} \kappa_{d,m})^2} [a_0 x_{os,1} + a_1 (1 - x_{os,1} \kappa_{d,m}) \tan x_{os,2} \\ &\quad + (1 - x_{os,1} \kappa_{d,m}) \kappa_{d,m}]. \end{aligned} \quad (41)$$

This stabilizes the first subsystem for the equilibrium point  $y_{os} = 0$ . With the relative degree of  $r = 2$  and the output derivatives, one defines a set  $\mathcal{Z}^*$  of  $\mathbf{x}_{os} \in \mathbb{R}^n$  that suffices

$$h(\mathbf{x}_{os}) = x_{os,1} = 0 \quad (42)$$

$$\mathcal{L}_{\mathbf{f}} h(\mathbf{x}_{os}) = (1 - x_{os,1} \kappa_{d,m}) \tan x_{os,2} = 0. \quad (43)$$

For practical reasons, it follows that  $x_{os,1} = x_{os,2} = 0$ . For this regime, we obtain a vector field

$$\mathbf{f}^*(\mathbf{x}_{os}) = \mathbf{f}(\mathbf{x}_{os}) - \mathbf{g}(\mathbf{x}_{os}) \frac{\mathcal{L}_{\mathbf{f}}^2 h(\mathbf{x}_{os})}{\mathcal{L}_{\mathbf{g}} \mathcal{L}_{\mathbf{f}} h(\mathbf{x}_{os})} \quad (44)$$

and finally, the zero dynamics  $\mathbf{x}'_{os} = \mathbf{f}^*(\mathbf{x}_{os})$  can be expressed

$$\begin{aligned} x'_{os,1} &= 0 \\ x'_{os,2} &= 0 \\ x'_{os,3} &= -\frac{v_2}{v_m D_1 L_2} [L_2 \sin(x_{os,3} + \phi_{d,1}) \\ &\quad - (D_1 + L_2 \cos(x_{os,3} + \phi_{d,1})) \tan \delta_1] \\ &\vdots \\ x'_{os,n} &= -\frac{v_m}{v_m D_{m-1} L_m} [L_m \sin(x_{os,n} + \phi_{d,m-1}) \\ &\quad - (D_{m-1} + L_m \cos(x_{os,n} + \phi_{d,m-1})) \tan \delta_{m-1}]. \end{aligned} \quad (45)$$

For the stability analysis, we linearize (45) around the equilibrium  $\mathbf{x}_{os} = \mathbf{0}$ . A Taylor linearization gives us a linear system that approximates the internal dynamics locally on that equilibrium point,

$$\tilde{\mathbf{x}}'_{os} = \mathbf{A}_Z \tilde{\mathbf{x}}_{os}. \quad (46)$$

Consequently, the jacobian matrix of the zero dynamics is

$$\mathbf{A}_Z = \left. \frac{\partial \mathbf{f}^*}{\partial \mathbf{x}_{os}} \right|_{\mathbf{x}_{os}=\mathbf{0}} = \begin{pmatrix} 0 & 0 & 0 & \cdots & 0 & 0 \\ 0 & 0 & 0 & \cdots & 0 & 0 \\ \vdots & \vdots & a_{33} & \ddots & \vdots & \vdots \\ \vdots & \vdots & 0 & \ddots & 0 & 0 \\ 0 & 0 & \vdots & \ddots & a_{n-1n-1} & 0 \\ 0 & 0 & 0 & \cdots & 0 & a_{nn} \end{pmatrix} \quad (47)$$

with the components

$$a_{i+2i+2} = -\frac{v_{i+1}}{v_m D_i} [\cos \phi_{d,i} + \sin \phi_{d,i} \tan \delta_i] \quad (48)$$

and  $i = 1, \dots, n-2$ .

The eigenvalues of the matrix  $\mathbf{A}_Z$  are easily obtained. The dynamics of the first subsystem is described by a double integrator, both eigenvalues are zero,  $\lambda_1 = \lambda_2 = 0$ . For the stability of the internal dynamics, the remaining  $n-r$  eigenvalues are of interest,

$$\lambda_i = -\frac{v_{i+1}}{v_m D_i} [\cos \phi_{d,i} + \sin \phi_{d,i} \tan \delta_i]. \quad (49)$$

By making use of the equilibrium relations (24), (25) and (27), and noting that for a steady state path movement the curvatures need to have the same sign, these eigenvalues can be simplified to

$$\lambda_i = -\frac{1}{D_i}. \quad (50)$$

The theorem of Hartman-Grobman states that the behavior of the nonlinear system (45) corresponds to the one of the linearized system (46) within a neighbourhood around the equilibrium, if the equilibrium point of the zero dynamics is hyperbolic. This is the case when the real part of the eigenvalues is different from zero.

The feedback (36) makes the equilibrium point  $\mathbf{x}_{os} = \mathbf{0}$  local asymptotic stable when the eigenvalues of the zero dynamics have negative real parts, i.e., are located in the left half of the complex plane.

This analysis shows that the hitch point positions need to be behind the axles,  $D_i > 0$ , greatly limiting the vehicle structures that this approach can stabilize.

We can therefore conclude that, with this algorithm, a stable controller for the nSNT case is obtained under the condition of positive hitch offsets,  $D_i > 0$ , being in consonance with the results from other publications, e.g. [10].

This means, that this control approach is not suitable for many vehicles with great practical importance, like semi-trailers, which have a  $D < 0$ , or road-trains, with one  $D = 0$ .

Finally, in order to control the vehicle, one propagates  $u_{os} = \tan \delta_{m-1}$  through the vehicle structure to compute the real steering angle  $\delta_0$  of the tractor. The complete algorithm steps will be shown in the next section for a tractor with two trailers.

#### IV. RESULTING CONTROL

Here, vehicles with  $D > 0$  conform the *nominal* case. *Special* cases of vehicles where  $D = 0$  or  $D < 0$  are not considered in this resulting control. The emphasis around *special* is from the view of the control problem, since actually these vehicles are the most common in real world applications. They will be analyzed in future publications.

Parting from (41), one needs to obtain the feedback for the kinematic vehicle model (1)-(4). The feedback depends on the offset values  $x_{os,1}$  and  $x_{os,2}$ , computed with (9) and (10), respectively, as well as the wheelbase  $L_m$  and the path curvature  $\kappa_{d,m}$ . The coefficients  $a_0$  and  $a_1$  are design variables and defined through (39) and (40).

Having the fictive system input  $u_{os} = \tan \delta_{m-1}$ , first we compute the desired rotational velocity for the last trailer,  $\omega_m$ , which is expressed as

$$\omega_m = \frac{v_m}{L_m} u_{os}. \quad (51)$$

Note that in this equation the translational velocity  $v_m$  is needed. It can be obtained from (6).

Finally, to compute the steering angle  $\delta_0$  for the front vehicle, the velocity propagation from the last trailer to the front vehicle is performed through (7). In this way, the feedback is expressed in original coordinates, i.e. the fixed frame model, and the system input  $\delta_0$  is obtained.

To show the stability of the closed loop system, a vehicle with two trailers for the *nominal* case is considered. With the system state introduced in Section II-A we have

$$\begin{aligned} \dot{x}_1 &= v_1 \cos x_3 \\ \dot{x}_2 &= v_1 \sin x_3 \\ \dot{x}_3 &= \frac{v_1}{L_1} \tan \delta_0 \\ \dot{x}_4 &= -\frac{v_1}{L_1 L_2} [L_1 \sin(x_4 - x_3) \\ &\quad + D_1 \cos(x_4 - x_3) \tan \delta_0] \\ \dot{x}_5 &= -\frac{v_1}{L_1 L_2 L_3} ([L_1 L_2 \sin(x_5 - x_3) \\ &\quad + D_1 L_2 \cos(x_5 - x_3) \tan \delta_0] \\ &\quad - (L_2 + D_2) \cos(x_5 - x_4) [L_1 \sin(x_4 - x_3) \\ &\quad + D_1 \cos(x_4 - x_3) \tan \delta_0]). \end{aligned} \quad (52)$$

The position of the last trailer is computed through (5) and the offset relations expressed in vehicle state and path variables result to

$$\begin{aligned} x_{os,1} = & -(x_1 - D_1 \cos x_3 - (L_2 + D_2) \cos x_4 \\ & - L_3 \cos x_5 - p_{d,1}) \sin \theta_d \\ & + (x_1 - D_1 \sin x_3 - (L_2 + D_2) \sin x_4 \\ & - L_3 \sin x_5 - p_{d,2}) \cos \theta_d \end{aligned} \quad (53)$$

and

$$x_{os,2} = \theta_{os} = x_5 + \pi - \theta_d. \quad (54)$$

The desired rotational velocity for the tractor can be expressed as

$$\begin{aligned} \omega_1 = & \frac{v_3}{D_1 D_2} [L_2 \cos(x_4 - x_3) \sin(x_5 - x_4) \\ & + L_2 \sin(x_4 - x_3) \cos(x_5 - x_4) \\ & + u_{os} (D_2 \sin(x_4 - x_3) \sin(x_5 - x_4) \\ & + L_2 \cos(x_4 - x_3) \cos(x_5 - x_4))] \end{aligned} \quad (55)$$

In that equation we need to substitute the instantaneous translational velocity of the last trailer

$$\begin{aligned} v_3 = & \frac{v_1}{L_1 L_2} [D_1 \tan \delta_0 (D_2 \cos(x_4 - x_3) \sin(x_5 - x_4) \\ & - L_2 \sin(x_4 - x_3) \cos(x_5 - x_4)) \\ & + L_1 D_2 \sin(x_4 - x_3) \sin(x_5 - x_4) \\ & + L_1 L_2 \cos(x_4 - x_3) \cos(x_5 - x_4)] \end{aligned} \quad (56)$$

and the feedback  $u_{os}$ . Finally, fitting everything into (52) we obtain the closed loop system

$$\dot{\mathbf{x}} = \mathbf{f}_{CL}(\mathbf{x}). \quad (57)$$

For the stability analysis, we will define a stationary regime to linearize the system about it. We consider a path on the  $x$  axis in positive direction. One obtains the stationary driving state with  $x_2 = 0$ ,  $x_3 = \pi$ ,  $x_4 = \pi$  und  $x_5 = \pi$ , as well as  $\kappa_{d,m} = 0$  and  $\theta_d = 0$  for the path. The initial errors fade away and therefore the offset values become  $x_{os,1} = 0$  and  $x_{os,2} = 0$ . The linearized system about this regime is

$$\dot{\hat{\mathbf{x}}} = \mathbf{A}_N \hat{\mathbf{x}} \quad (58)$$

where  $\mathbf{A}_N = (\mathbf{a}_{N,1}, \mathbf{a}_{N,2}, \mathbf{a}_{N,3}, \mathbf{a}_{N,4}, \mathbf{a}_{N,5})$  is the Jacobian matrix. Its columns are

$$\mathbf{a}_{N,1} = \mathbf{0}, \quad (59)$$

$$\mathbf{a}_{N,2} = \begin{pmatrix} 0 \\ 0 \\ \frac{a_0 L_2 L_3}{D_1 D_2} v_1 \\ -\frac{a_0 L_3}{D_2} v_1 \\ a_0 v_1 \end{pmatrix}, \quad (60)$$

$$\mathbf{a}_{N,3} = \begin{pmatrix} 0 \\ -v_1 \\ \frac{a_0 D_1 L_2 L_3 + D_2}{D_1 D_2} v_1 \\ -\frac{a_0 D_1 L_3}{D_2} v_1 \\ a_0 D_1 v_1 \end{pmatrix}, \quad (61)$$

$$\mathbf{a}_{N,4} = \begin{pmatrix} 0 \\ 0 \\ \frac{(L_2 + D_2) a_0 L_2 L_3 - L_2 - D_2}{D_1 D_2} \\ -\frac{((L_2 + D_2) a_0 L_3 - 1) v_1}{D_2} \\ (L_2 + D_2) a_0 v_1 \end{pmatrix}, \quad (62)$$

$$\mathbf{a}_{N,5} = \begin{pmatrix} 0 \\ 0 \\ \frac{a_0 L_2 L_3^2 + a_1 L_2 L_3 + L_2}{D_1 D_2} v_1 \\ -\frac{a_0 L_3^2 + a_1 L_3 + 1}{D_2} v_1 \\ (a_0 L_3 + a_1) v_1 \end{pmatrix}, \quad (63)$$

The eigenvalues of that Jacobian matrix are computed from the zeroes of its characteristic polynomial

$$\begin{aligned} 0 = & \det(s\mathbf{I}_5 - \mathbf{A}_N) \\ = & -\frac{s(v_1 - D_1 s)(v_1 - D_2 s)(a_0 v_1^2 - a_1 v_1 s + s^2)}{D_1 D_2}, \end{aligned} \quad (64)$$

resulting in

$$\begin{aligned} s_1 &= 0, \\ s_2 &= \frac{v_1}{D_1}, \\ s_3 &= \frac{v_1}{D_2}, \\ s_4 &= \frac{a_1 - \sqrt{a_1^2 - 4a_0}}{2} v_1, \\ s_5 &= \frac{a_1 + \sqrt{a_1^2 - 4a_0}}{2} v_1. \end{aligned} \quad (65)$$

From the movement of the vehicle on the  $x$  axis,  $x_1$  grows continuously and therefore the first eigenvalue is  $s_1 = 0$ . The interesting eigenvalues are the remaining ones. Since  $v_1 < 0$  for backward motion,  $s_2$  and  $s_3$  are only in the left complex half plane if  $D_1, D_2 > 0$ . This was already the stability condition of the offset system. The eigenvalues  $s_4$  and  $s_5$  depend on the coefficients  $a_0$  and  $a_1$ , as well as the velocity  $v_1$ . Selecting a double real negative design eigenvalue  $s = s_1 = s_2$  in (39) and (40), the above expressions result in

$$\begin{aligned} s_4 &= -s v_1, \\ s_5 &= -s v_1, \end{aligned} \quad (66)$$

and therefore they lay in the left complex half plane. This shows that the closed loop system is stable for this driving regime. The behaviour of this system on different path segments will be analyzed in the simulation section.

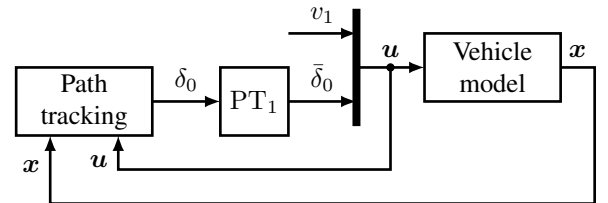
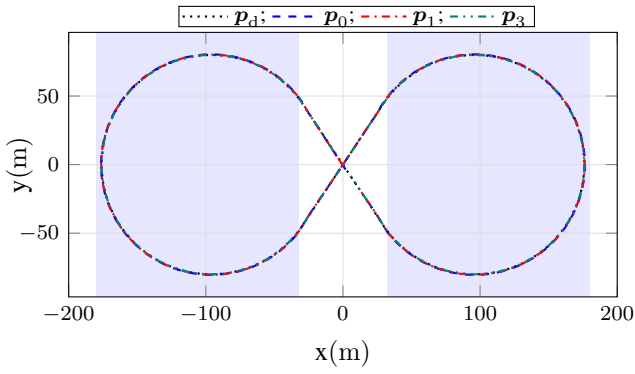


Fig. 5. Block diagram of the resulting simulation


 Fig. 6. Path and vehicle axle center positions in  $xy$ -Plane, case PC1.

## V. SIMULATION RESULTS

A series of simulations were performed in order to verify the results and evaluate the performance of the control law. To approximate the actuator dynamics, a first order delay with time constant  $T = 0.25$  s was interposed between the control output and the vehicle model input. This delayed steering angle is denoted as  $\bar{\delta}_0$ . The control system was tested for a vehicle with two trailers with the dimensions  $L_1 = 4$  m,  $L_2 = L_3 = 5$  m and  $D_1 = D_2 = 1$  m and the constraint  $|\delta_{0,\max}| = \pi/4$ . Fig. 5 shows the simulation setup.

Common scenarios for testing the performance are straight lines with initial error or eight-shaped curves, to show the behavior with varying curvature. A straight path scenario with different design poles was previously discussed in [8]. In this contribution we will focus on a more dynamic path to show the influence of varying curvature on the control performance. The path considered is an eight-shape composed of two circles with radius 80 m and circle centers'  $x$ -coordinates  $\pm 1.2 \cdot 80$  m  $= \pm 96$  m, connected through the inner tangents. That implies the path curvature not to be continuous, i.e. there are curvature steps for the path in the transitions circle-straight segment and viceversa. To evaluate the simulation results, it is essential to keep this disturbance in mind. The desired path starts at  $(0,0)$  in the direction of the second quadrant and is shown in Fig. 6. Highlighted regions are the curved path segments. From (38) we obtain the stabilizing coefficients  $a_0 = s_1 s_2$  and  $a_1 = -(s_1 + s_2)$ . Two combinations were tested, PC1 with  $s_1 = s_2 = -0.1$  and PC2 with  $s_1 = s_2 = -0.2$ .

The initial position of the vehicle shows backwards in path direction with an initial off track error. Path tracking performance for both poles is analyzed at a driving speed of  $v_1 = -1.4$  m/s. The path with the resulting movement of the vehicle axle centers, excluding  $p_2$  to not overload the plot, is shown in Fig. 6. An examination of the curves shows clearly that the control law drives the vehicle along the path.

In Fig. 7 one can observe that it reduces the off-track distance as well as the orientation error. The *jack-knife* phenomenon, i.e. the folding of the vehicle bodies, is prevented as well, since the relative orientations are kept  $\phi_1, \phi_2 \ll \pi/2$ .

The curved segments are highlighted and between  $t_1 \approx 25$  s

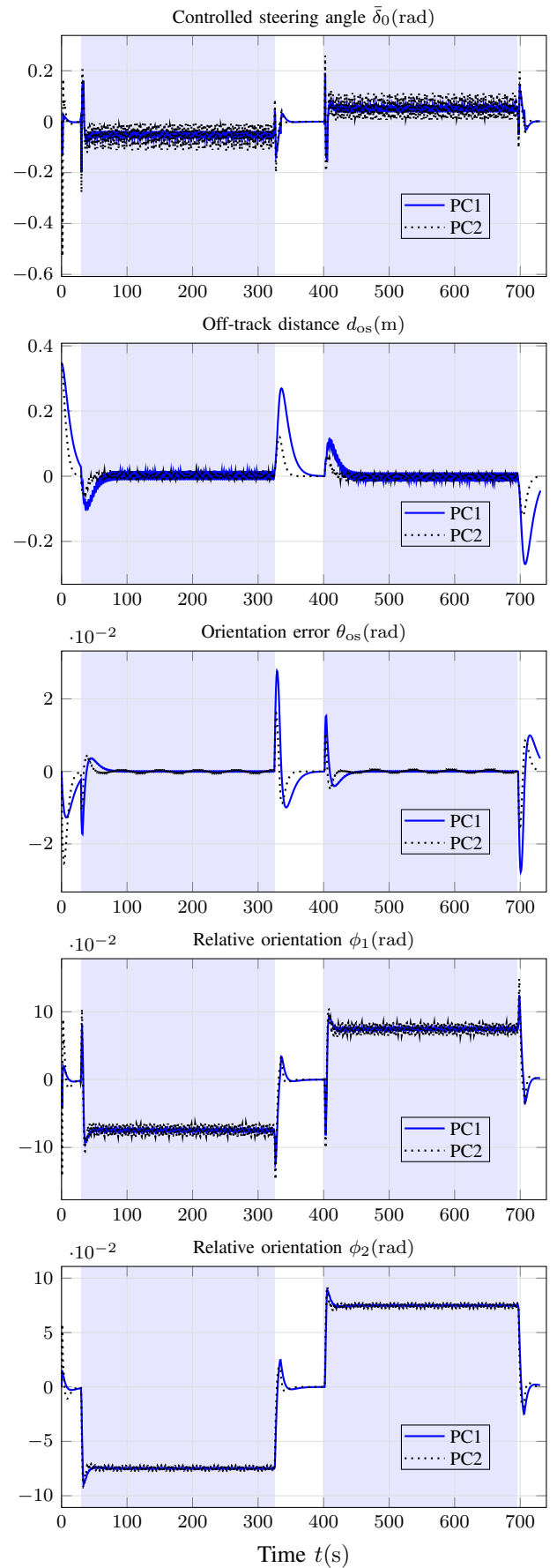


Fig. 7. Vehicle behavior in backward eight-shaped path following

and  $t_2 \approx 325$  s as well as  $t_3 \approx 400$  s and  $t_4 \approx 700$  s. At these points in time, the transition between zero curvature and some value different from zero (and viceversa) occurs, introducing errors. This results in visible error jumps through all curves. Although this curvature discontinuities were not considered in the control algorithm, the vehicle is guided quickly back to the path proximity and the errors are reduced successfully.

The steering angle shows an expected behaviour, in order to follow the straight and curved path segments with the last trailer. E.g. for the steady state in the curve segments it reaches a quasi-constant value for PC1, while having similar behaviour but more signal amplitude with PC2. With greater absolute value of the poles, errors cause bigger control actions. Steering action for transitioning between path segments with different curvatures is visible at the mentioned times.

Considering the application on a real actuator, although the goal is to minimize the distance and orientation error to the path, which are kept smaller with PC2, the mentioned chattering is not acceptable and the pole combination PC1 is preferred.

## VI. CONCLUSIONS

In this paper, path tracking in backward motion based on the exact linearization of a truck with N trailers was reviewed. For the case of a non-Standard N-Trailer (nSNT) with positive hitch point positions  $D > 0$  only, a stable controller was found and its performance was successfully tested in a simulation for two trailers. Nevertheless, the limitation regarding the hitch point position excludes important real road vehicle types. Therefore, relaxing the structural vehicle limitations by overcoming the unstable zero dynamics is the key subject of upcoming research.

Based on the results found in this paper, a promising approach is to convert the real vehicle into a virtual one that keeps the condition  $D > 0$  and apply the stabilizing control law on that virtual vehicle. Afterwards, the found control is converted back into the real vehicle steering angle. The goal for upcoming publications is to show that the adapted control algorithm is able to guide real world vehicle types, such as semi-trailers ( $D < 0$ ) and road-trains ( $D = 0$ ).

Furthermore, the algorithms will be verified further on different paths in simulation and in an automated vehicle laboratory, the Fraunhofer IVI *DriveLab* previously presented in [21]. It includes vehicles of the semi-trailer type and shows the influence of noise and actuator dynamics. This demonstrator allows to test driving algorithms in a secure and replicable environment.

After successful trials in the *DriveLab*, the application on a real automated 18 t truck, the Fraunhofer IVI *AutoTruck*, is planned. While this truck is capable of driving autonomously, the missions are planned and managed on an online yard automation software called *helyOS*, presented in [22].

In addition, aspects such as input saturation or mechanical limitations like the maximum relative angle between two vehicle parts so as not to collide should be considered before the implementation in real world applications, e.g. [5], [23].

## REFERENCES

- [1] M. Riesmeier, O. Schnabel, F. Woittennek, and T. Knüppel, "Zur Folgeregelung mehrachsiger Fahrzeuge," *at - Automatisierungstechnik*, vol. 64, no. 8, 2016.
- [2] C. Altafani, "The general n-trailer problem: conversion into chained form," in *Proceedings of the 37th IEEE Conference on Decision and Control (Cat. No.98CH36171)*. IEEE, 1998.
- [3] P. Rouchon, M. Fliess, J. Levine, and P. Martin, "Flatness, motion planning and trailer systems," in *Proceedings of 32nd IEEE Conference on Decision and Control*. IEEE, 1993.
- [4] M. Sampei, T. Tamura, T. Kobayashi, and N. Shibui, "Arbitrary path tracking control of articulated vehicles using nonlinear control theory," *IEEE Transactions on Control Systems Technology*, vol. 3, no. 1, pp. 125–131, 1995.
- [5] M. Werling, M. Heidingsfeld, P. Reinisch, and L. Gröll, "Assistiertes und automatisiertes Rückwärtsrangieren mit Anhänger," *at - Automatisierungstechnik*, vol. 62, no. 1, 2014.
- [6] B. d'Andréa Novel, L. Menhour, M. Fliess, and H. Mounier, "Some remarks on wheeled autonomous vehicles and the evolution of their control design," *IFAC Proceedings Volumes*, 2016.
- [7] M. M. Michalek, "A highly scalable path-following controller for n-trailers with off-axle hitching," *Control Engineering Practice*, vol. 29, pp. 61–73, 2014.
- [8] J. Kolb, G. Nitzsche, S. Wagner, and K. Robenack, "Path Tracking of Articulated Vehicles in Backward Motion," in *2020 24th International Conference on System Theory, Control and Computing (ICSTCC)*. IEEE, 2020.
- [9] P. Bolzern, R. DeSantis, A. Locatelli, and D. Masciocchi, "Path-tracking for articulated vehicles with off-axle hitching," *IEEE Transactions on Control Systems Technology*, vol. 6, no. 4, pp. 515–523, 1998.
- [10] P. Bolzern, R. M. DeSantis, and A. Locatelli, "An input-output linearization approach to the control of an n-body articulated vehicle," *Journal of Dynamic Systems, Measurement, and Control*, vol. 123, no. 3, pp. 309–316, 2001.
- [11] R. DeSantis, "Path-tracking for articulated vehicles via exact and jacobian linearization," *IFAC Proceedings Volumes*, vol. 31, no. 3, pp. 159–164, 1998.
- [12] R. DeSantis, J. Bourgeot, J. Todeschi, and R. Hurteau, "Path-tracking for tractor-trailers with hitching of both the on-axle and the off-axle kind," in *Proceedings of the IEEE International Symposium on Intelligent Control*. IEEE, 2002.
- [13] J. Morales, J. L. Martinez, A. Mandow, and A. J. Garcia-Cerezo, "Steering the last trailer as a virtual tractor for reversing vehicles with passive on- and off-axle hitches," *IEEE Transactions on Industrial Electronics*, vol. 60, no. 12, pp. 5729–5736, 2013.
- [14] D. A. Lizárraga, P. Morin, and C. Samson, "Exponential Stabilization of Certain Configurations of the General N-Trailer System," INRIA, Tech. Rep. RR-3412, 1998.
- [15] M. Werling and L. Groll, "Low-level controllers realizing high-level decisions in an autonomous vehicle," in *2008 IEEE Intelligent Vehicles Symposium*. IEEE, 2008.
- [16] A. Isidori, *Nonlinear Control Systems*. Springer London, 1995, ISBN: 978-1-4471-3909-6.
- [17] K. Röbenack, *Nichtlineare Regelungssysteme*. Springer Berlin Heidelberg, 2017, ISBN: 978-3-662-44091-9.
- [18] —, "On the Direct Computation of the Byrnes-Isidori Normal Form," *PAMM*, vol. 17, no. 1, pp. 811–812, 2017.
- [19] —, "Computation of multiple Lie derivatives by algorithmic differentiation," *Journal of computational and applied mathematics*, vol. 213, pp. 454–464, 2008.
- [20] F. Svaricek, "Nullodynamik linearer und nichtlinearer Systeme: Definitionen, Eigenschaften und Anwendungen," *at - Automatisierungstechnik*, vol. 54, 2006.
- [21] J. K. Kolb, G. Nitzsche, and S. Wagner, "A simple yet efficient path tracking controller for autonomous trucks," *IFAC-PapersOnLine*, vol. 52, no. 8, pp. 307–312, 2019.
- [22] G. Nitzsche, S. Wagner, and N. Belov, "helyOS – Highly Efficient Online Yard Operating System," in *Commercial Vehicles 2019*. VDI Verlag, 2019, pp. 329–338.
- [23] J. Morales, J. L. Martinez, A. Mandow, and I. J. Medina, "Virtual steering limitations for reversing an articulated vehicle with off-axle passive trailers," in *2009 35th Annual Conference of IEEE Industrial Electronics*. IEEE, 2009.